Spring 2019

Acoustoelastic Metamaterial with Simultaneous Noise Filtering and Energy Harvesting Capability from Ambient Vibrations

Fariha Mir

ACOUSTOELASTIC METAMATERIAL WITH SIMULTANEOUS NOISE FILTERING AND ENERGY HARVESTING CAPABILITY FROM AMBIENT VIBRATIONS

by

Fariha Mir

Bachelor of Science
Military Institute of Science and Technology, Bangladesh, 2014

Submitted in Partial Fulfillment of the Requirements

For the Degree of Master of Science in

Mechanical Engineering

College of Engineering and Computing

University of South Carolina

2019

Accepted by:

Sourav Banerjee, Director of Thesis

Victor Giurgiutiu, Reader

Cheryl L. Addy, Vice Provost and Dean of the Graduate School

DEDICATION

This work is dedicated to my parents Mir Imdadul Haque and Syeda Afsana Ahsan. I would also like to dedicate it to my husband Ahmed Shehab Khan.

ACKNOWLEDGMENTS

I would like to express my sincere appreciation and respect to my advisor Dr. Sourav Banerjee for his cordial support and valuable advice in my research. I also would like to thank all the members of iMAPS for their continuous help and support. Finally, I would like to thank my husband and my parents for their support, constant encouragement and unconditional love to me.

ABSTRACT

Harvesting unused and untapped energy from ambient vibration noise and acoustic sound waves is an emerging field of research in the recent years. Utilization of the energy with a wide band of the frequency spectrum from the vibrational sources alone stands as one of the most promising ways to power small electronic devices, smartphones, local structural health monitoring (SHM) sensors and home and workshop appliances. Various sources of ambient vibration and acoustic noise can be found around us in our everyday life. These sources are abundant in almost all the engineering industries and manufacturing facilities for example in aerospace, mechanical and civil sectors. Running machinery in a workshop, ambient vibration in a manufacturing facility, vibrating wings of an aircraft, high dB aircraft noise near airports, engine noise in a plant, vehicle noise near a roadside facility, etc. are few examples of the ambient source of energy that can be harvested which are otherwise wasted. If a suitable mechanism is devised, the vibration and acoustic noise sources can be tapped and equipped to reclaim the energy to create local power sources. First, in this thesis, a recently proposed method of creating Acoustoelastic Metamaterial (AEMM) is used to investigate further if that can be used to harvest energy from the industrial noise barriers. It is known that the noise barriers are designed to minimize the noise outside the boundary like we see the noise barriers beside the highways. Construction materials like concrete, steel, vinyl, wood or earth mounds are used in the industrial sound barriers that can reduce the sound pressure level (dB) on the other side of the barrier. In this thesis, a novel metamaterial wall (MetaWall) is proposed to redefine the industrial

sound isolation wall using the integrated AEMM units. Purpose of the proposed MetaWall is to deliver two principal objectives, simultaneously, 1) provide enhanced sound isolation capability, which is closer to ~1.5 times the current state-of-the-art, and 2) make use of the isolated noise by transforming into usable electrical energy. Acoustic metamaterials are traditionally reported for guiding and isolating acoustic and elastic waves. In this article, wave isolation and energy harvesting capabilities of the acoustic metamaterial is fused to propose MetaWall unit bricks, which are made of rubber-metal-concrete composite, as an industrial building material. A numerical study shows that the designed prototype of a MetaWall brick can generate up to ~2mW of power against 10KΩ resistive load with just only 1 mm displacement depending on the type of smart material used in the composite while maintaining compressive strength greater than the minimum required strength 5 MPa. Such acousto-elastic metamaterial (AEMM) models can also be used in the aerospace sector to power the NDE/SHM sensors. Hence, further in this thesis, a rigorous study is made to find the required power to use traditional NDE / SHM sensors such that the power can be harvested with the AEMM model. The ultimate goal of this second study is to minimize the size of the proposed AEMM model to make it suitable for aerospace applications. With the change of the materials of the cell constituents, it is shown that the power outputs from a similar model can be significantly altered and further optimized (not performed in this thesis). A parametric study is performed to show the change in the output power pattern. A plate type metamaterial is proposed to harvest a significant amount of energy from the ambient vibration as low as 100Hz.

TABLE OF CONTENTS

LIST OF TABLES

LIST OF FIGURES

LIST OF ABBREVIATIONS

AESC…… Acousto Elastic Sonic Crystal

AEMM……. Acousto Elastic Meta-Material

FEM……. Finite Element Method

PVDF……. Polyvinylidene Fluoride

PVC…… Polyvinyl Chloride

PZT……. Lead Zirconate Titanate

SC.....Sonic Crystal

CHAPTER 1

INTRODUCTION

1.1 Background and motivation

Energy is a vital element in the growth of modern society. From a light bulb to outer space missions, we need energy everywhere. Some energy is visible to us, such as light, but most of the existing energies in nature are not visible. Among all these, electric energy is the mostly used form. Due to the high demand for electricity, measures are being taken to convert other forms of energy to electricity. The process which derives energy from external sources is called Energy Harvesting. Converted energy can be stored in a capacitor or battery for later use. Energy harvesters provide power for low energy electronics.

Interest in converting ambient vibration energy into power has increased dramatically in the last few years[1-3]. The goal of such research is to power wireless remote sensors which are usually powered by batteries. Batteries have a finite lifespan which creates problems with frequent replacement during emergencies. If ambient energy in the atmosphere can be utilized to harvest energy to power these batteries simultaneously, then most of the existing problems could be solved. There are various transduction mechanisms that can be employed to harvest such kind of energy. One of that is the use of piezoelectric materials to harvest energy from the unused or lost vibration energy of the host structure.

Not only ambient vibration but also the sound and noise created by the modern machinery and vehicles can be used to harvest energy by trapping them in a medium. In recent years road traffic has increased tremendously. It is without any doubt, one of the most widespread sources of noise annoyance. Industries with heavy machinery also introduce a significant amount of noise into the atmosphere. Acoustic noise barriers can be developed to reduce this noise pollution. But the efficiency of these barriers is a question for a long time. Researchers are working to improve the efficiency but till now the maximum reported an efficiency of the noise barriers is around ~50%[4].

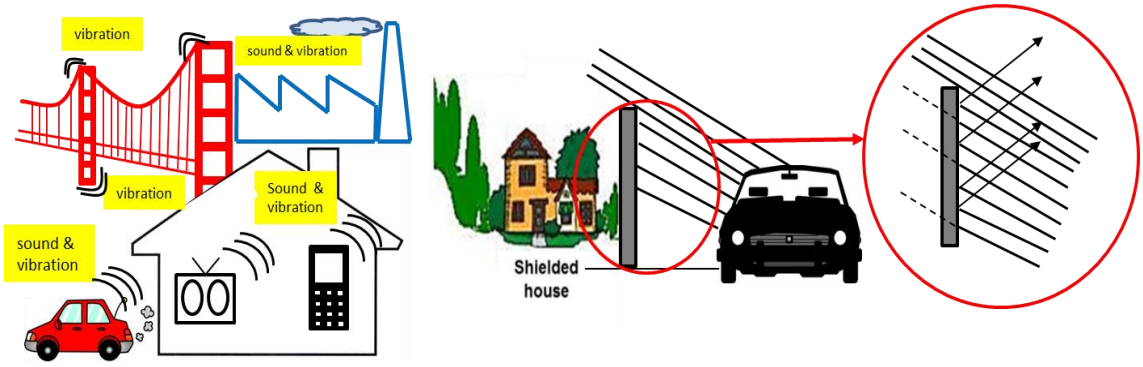

Figure-1.1: Sources of unused ambient sound and vibrations

With respect to the traditional industrial barriers, new materials and designs are combined to create a more effective system [5]. Sound absorbing materials are being used to trap the sound inside the material and decrease the reflection of noise. But this trapped energy is not being used anywhere. If this trapped acoustic energy can be used in certain ways, then it can be a source of harvesting energy too.

These vehicles and machinery create vibration also. The movement of the cars on the roads create both sound and vibration. The machines have their own frequency of

vibration too. These abandoned vibration energies can be utilized in the energy harvesting field. In order to get the most of it, maximum number of sources must be utilized. Most important is to develop an effective system for this method.

1.2 Problem statement and objective

The objective of this thesis is to develop a novel metamaterial based Acousto-Elastic Meta-material(AEMM) with controlled geometric features which can trap low frequencies. These sonic crystals can be used to develop noise barriers with higher efficiency than the prevailing traditional ones. This work also investigates the scope of using the trapped energy inside the cells. The trapped energy can be transferred as electricity using proper transduction method. Modification of the AEMM to harvest the maximum amount of energy is presented herein.

Most studies do not provide the experimental validation for their model, may be for design complexity. Hence, these are unreliable for industrial implementation. In this thesis, the proposed concept has been experimentally verified.

Miniaturization is the trend these days. So, studies have been conducted to decrease the dimension of energy harvesting model while increasing the power output. A plate type model with different piezoelectric material is proposed to effectively harvest the ambient energy. This thesis evaluates and compares the proposed models and their direct intermediate and long-term development.

CHAPTER 2

LITERATURE REVIEW

Recent advancements in low power electronic gadgets, micro electromechanical systems and wireless sensors have significantly increased the local power demand. To circumvent the energy demand, low power local energy harvesters are proposed for harvesting energy from different ambient energy sources. Energy harvesters utilize the ability of piezoelectric materials to generate electric potential in response to external mechanical deformation. Significant research activities on low power energy harvesters can be found in many literatures. Key of these research activities are to introduce self-powered wireless electronics systems such that the maintenance, replacement of the old batteries and the chemical waste from conventional batteries could be avoided

2.1 Noise Reduction using Metamaterial

These days, with the development of transportation system, and tremendous increase in the traffic density, noise problem has drawn more attention in recent years. The impact of urban noise on the quality of life has become an important index to make both urban and environmental policy throughout the world [6]. Hence, different measures have been taken to minimize the roadside noises. Noise barriers are being used beside the roads to minimize the intensity of the generated noise. Researches have shown in certain noise barriers that under carefully controlled measurement conditions, the noise pattern changes with the panel types being absorptive to reflective[7]. Some studies have also showed that

some noise barriers create annoying sounds compared to areas without noise barriers which lead to low annoyance-reduction efficiency [8]. In most of the cases, the incident waves get reflected from the noise barriers. Collision of these reflected waves with the incident waves create such annoying sound. The problem is so acute that people have started thinking about alternative ways to create noise barriers. Some passive barriers (such as Median noise barriers), can be employed to reduce the impact of traffic noise on roadside communities via the direct propagation path[9]. To introduce passive barriers, two different absorbent materials including fibrous material and a grass surface are similarly being applied. Results from the use of these passive noise barriers show that thin absorptive barriers are equivalent at lower frequencies but perform better at mid to high frequencies compared to the rigid noise barriers[10]. However, when the barriers are placed in parallel and on opposite sides of a sound source, their performance deteriorates remarkably. Another study has shown that, addition of perforated sheet inside the wall improves the performance of the barriers [11].

Acousto-Elastic Sonic Crystals (AESC) possess unique properties that are not easily demonstrated by naturally occurring materials, such as, negative bulk modulus, negative mass density[12] AESC's are traditionally designed for guiding and filtering acoustic waves using the Bragg Scattering and Local Resonance phenomena [13]. These sound absorbing materials as noise barriers are not only required for the industrial purpose but also required for the building and residence applications. Components of usual building materials such as bricks or concrete are certified with required strength, specifically depending on their application. Moreover, the beauty enhancing sound absorbing materials are also used on with building materials to make the buildings sound resistant. Thus, if the

conventional building materials can be replaced by the sound absorbing acousto-elastic metamaterials(AEMM), the efficiency of the sound isolation process can be improved. On top of the capability of isolating sound, if the acousto-elastic metamaterials are used for building the structures, the prospect of harvesting energy from a building material will open a way to produce energy from the unused ambient energies. Hence, in this work, a proposal is made to create a acousto-elastic MetaWall brick as a building material that will not only absorb the ambient noise but also harvest the trapped noise to convert it to the electrical power. To meet these functions, the multi-functional MetaWall noise barriers are proposed to construct with Acousto-Elastic metamaterials (AEMM). AEMM is a kind of metamaterial, which is traditionally used for guiding and manipulating elastic waves. Based on the spectrum analysis of traffic at a different location it was shown[14] that the sound pressure decreases with increasing frequency especially above 1 KHz. Also, it was found[14, 15] that the 200 Hz – 500 Hz is the most frequently occurring frequency in the roadside noises where sound pressure is significant enough to cause harm to the human ear and may cause psychological trauma and other health diseases. Researchers designed many roadside sound barriers specifically to filter those low frequencies. Hence, in this article, the study is focused on the frequency range below 500 Hz (between ~420 - ~480 Hz) to filter the noise and harvest the energy from that specified range of frequency.

2.2 Energy Harvesting with Metamaterial

While traditional noise walls filter acoustic energy, these abounded filtered energy remains unused. Since the AEMM possess the capability to trap the filtered energy, it delivers the opportunity to recover these energies into a usable form. The review on energy harvester research shows that microcantilever energy harvesters are the most common low

power energy harvesters so far. For this kind of energy harvesters, the range of power outputs is in micro Watts[16-19]. Most of the energy harvester uses the local resonance physics to harvest dynamic energy. Acoustoelastic metamaterial (AEMM) can introduce local resonance in the structure. Recently AEMM's are introduced in the field of energy harvesting because of its unique ability in wave manipulation in a wide range of frequency[19-23]. It is established that sonic crystals have the ability to create frequency band gaps either through Bragg scattering or local resonance [24-26]. Hence several researchers proposed AEMM's for performing duel operations, filtering sound and harvesting trapped energy, simultaneously. This goal cannot be achieved using the usual energy harvesters available.

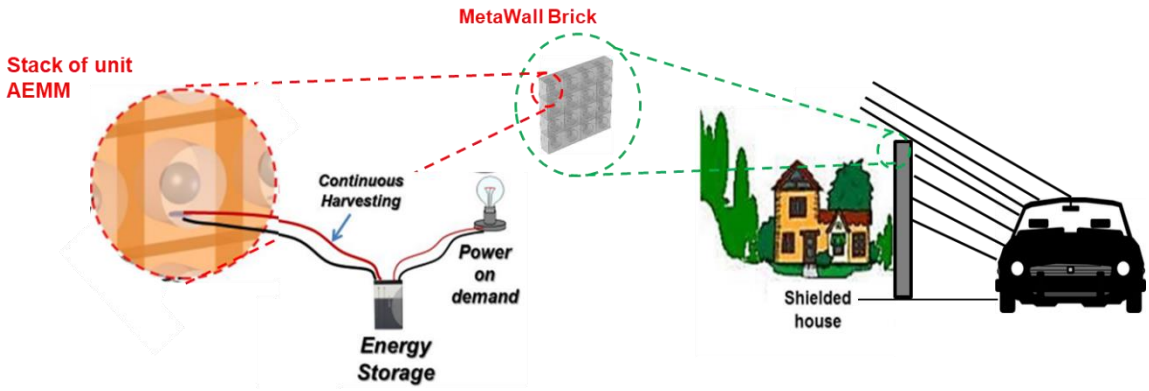

Figure-2.1: Schematic diagram of simultaneous noise control and energy harvesting using AEMM

The possibility of simultaneous wave filtering and energy harvesting was first mentioned by Gonella et al. [20] in 2009. Earlier, it has been proposed that [27-32] if the filtered wave energy at the stop band frequencies are trapped inside the soft constituent of the metamaterial as dynamic strain energy, then it must be possible to recover that same

energy using embedded piezoelectric wafers. Hence, coupling two different physics in a single phenomenon the bimodal AEMM is proposed. Maximum power can be harvested while the piezoelectric wafer is strained inside the matrix due to the local resonance of the embedded mass[28].

Earlier researchers have done various investigations on metamaterials that work in a dual mode where noise filtering and energy harvesting are done simultaneously. Ahmed et. al [29] have shown that at frequencies lower than ~3KHz can be trapped inside AEMM cell. The trapped energy can also be harvested using proper piezoelectric materials. However, the maximum power output from this model was in µW range.

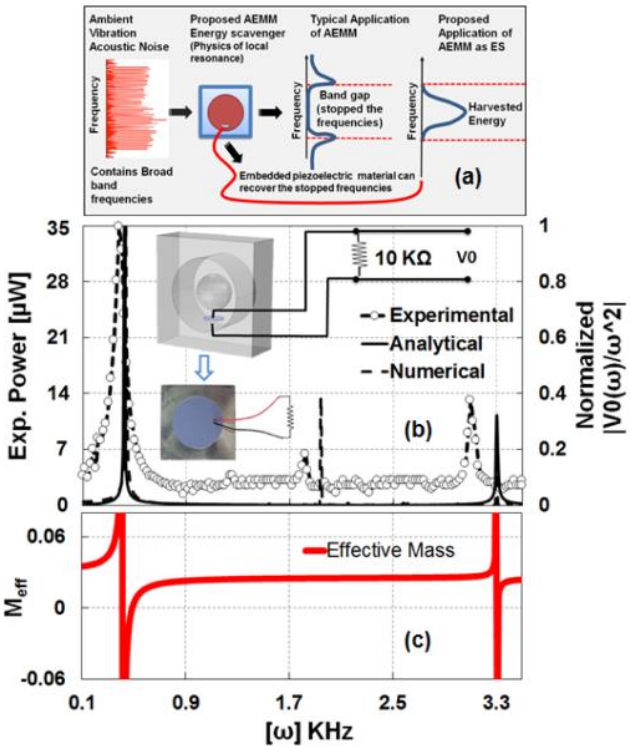

Figure- 2.2: Model representation and power output from the model used by Ahmed et.al

Since Acousto-elastic metamaterial (AEMM) possesses similar physics as AESC and AEMM can be an ideal choice harvest energy from the filtered wave energy. Till now energy harvesting capabilities of AEMM hasn't been explored extensively. In an ideal world, AEMM's are represented as a spring-mass combination in a mass-in-mass system. In this thesis, similar AEMM's are studied to develop low-frequency energy harvester. Very few attempts have been made so far to model the energy harvester based on Acousto-elastic metamaterials.

CHAPTER 3

AEMM MODEL DEVELOPMENT

3.1 Development of the Metamaterial

Traditionally, unit cell AEMM with specific geometric configuration and loading condition is able to provide local resonance at a unique frequency. A unit cell AEMM is shown in Fig. 3.1(b). The unit cell (dimension: 38mm X 38 mm X 25 mm) consists of a cylindrical matrix which is encapsulated in a concrete frame. A spherical heavy core made of lead is housed inside the matrix. The diameter of the core mass and the matrix are ∼12.5 mm and ∼25 mm, respectively. Mechanical properties of the cell constituents can be found in Table 3.1. This unit cell is proposed to be used as the building material for the sound absorbing MetaWall. A MetaWall brick without the embedded piezoelectric material was separately made to decommission and the compressive strength of the brick was found to be ~6.25 MPa. To demonstrate the concept of the proposed MetaWall, a three-dimensional model with 16-unit AEMM cells is considered as shown in Fig. 3.1(a).

Hence, the MetaWall is a stack of the unit cell with consistent geometric and mechanical configurations. Though in this article, MetaWall's capability with a specific acoustic frequency is tested, MetaWall with varied unit cell configurations can perform a similar operation within a broad spectrum of noise.

Table 3.1: Material properties of the cell constituents

Material	Density (kg/m^3)	Young's Modulus (Pa)	Poisson's ratio
Rubber	1600	0.9942e6	0.47
Concrete	2010	11.2e09	0.20
Lead	11340	13.5e09	0.43

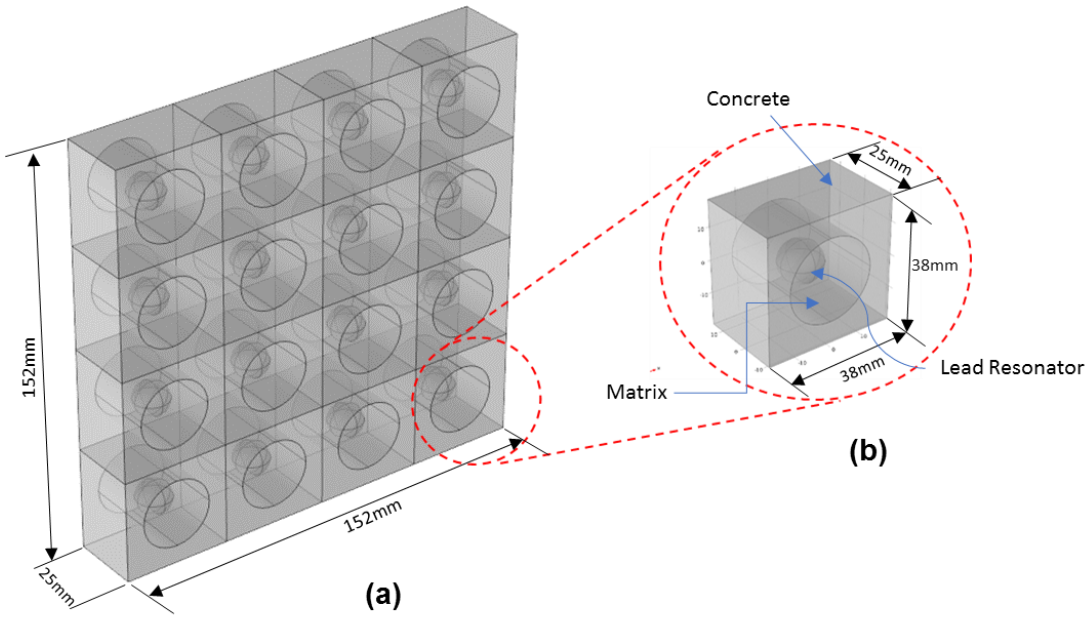

Figure-3.1: (a) 3D view of the wall with 16 cells; (b) unit cell of the wall

Since the proposed MetaWall brick consists of a series of AESC cells, the brick has the capability of harvesting energy trapped inside, while filtering the acoustic noises through the composite. To harvest energy, the proposed MetaWall is modified by placing piezoelectric materials inside the unit cell of AESC by judicially analyzing the vibration mode of the soft constituents. Two different type of piezoelectric materials were analyzed

a) ceramic Lead Zirconate Titanate (PZT) wafer and b) polymer Polyvinylidene Fluoride (PVDF) film. Both materials were first compared with different configurations. To keep the resonance frequency below 500 Hz one specific orientation was adopted as discussed in the subsequent sections.

Two arrangements of MetaWall are proposed in this work. Those are 1) concrete free surface and 2) matrix free-surface arrangements (refer chapter 5 for details). In the concrete free surface arrangement, the MetaWall has been placed in such a way that the concrete frame of each unit cell remains free and encounters direct acoustic incidence. Since a multi-layered MetaWall is more practical for industrial application, only the front or the first layer of the concrete free surface will encounter the dynamic excitation. In case of the matrix free-surface arrangement, the unit-cell MetaWall is rotated, and the matrix constituent of the cell will remain free and will be exposed to the sound. In a multi-layered matrix free-surface arrangement, the single and double capping configurations are envisioned to enhance the local and global power output. Additionally, a reasonable gap is considered in between two adjacent layers in case of single cover design. Detailed reasoning behind such proposals can be found in Chapter 5. Finally, the proposed MetaWall was fabricated, and energy harvesting capability was tested numerically and experimentally.

CHAPTER 4

AEMM MODEL AS NOISE BARRIER

4.1 AEMM MetaWall as Noise Barrier

In this study, an arbitrary frequency of ~460 Hz(<500Hz) is considered to filter and test the acoustic noise filtration capability of the unit cell AEMM. Finite element analysis tool (COMSOL Multiphysics) was used in this work to investigate the target objective. Since energy trapping is the key in filtering acoustic waves using AEMM, it is crucial to have local resonance phenomena in the unit cell AEMM at the frequency of interest (~460 Hz). To investigate the existence of local resonance modes around ~460Hz, dispersion curve of the unit cell is computed. To numerically compute the dispersion relation the unit cell is considered infinite both in x- and y-directions by arranging the unit cell periodically. Bloch–Floquet periodic boundary conditions [24] are applied at all boundaries of the unit cell. The Bloch–Floquet boundary conditions are based on the Floquet theory which can be applied to the problem of small-amplitude vibrations of spatially periodic structures. The dispersion curve of the unit cell is shown in Fig. 4.1(a). Two flat bands can be observed in the proximity of ~461 Hz, which denotes local resonance at corresponding frequencies. To identify the existence local resonance frequency more convincingly, Density of States (DOS) are computed at each frequency within the frequency range of 300-500 Hz. DOS of the system is the number of states (modes) that exists at each frequency level. A high DOS

at a specific frequency level means that there are multiple modes available for occupation. Maximum DOS can be obtained where the frequency band is almost straight in the dispersion curve, which means the group velocity is close to zero and the wave energy is trapped inside the structure. Zero DOS at any frequency means that at that frequency no modes could occupy any level (termed as stop band) of the energy. For highly dispersive unimodal wave motion, the DOS is very small but not zero. DOS is calculated from the dispersion relation by applying the relation

$$DOS(\omega) = \frac{1}{\pi}\left({}^{dk}/_{d\omega}\right)$$

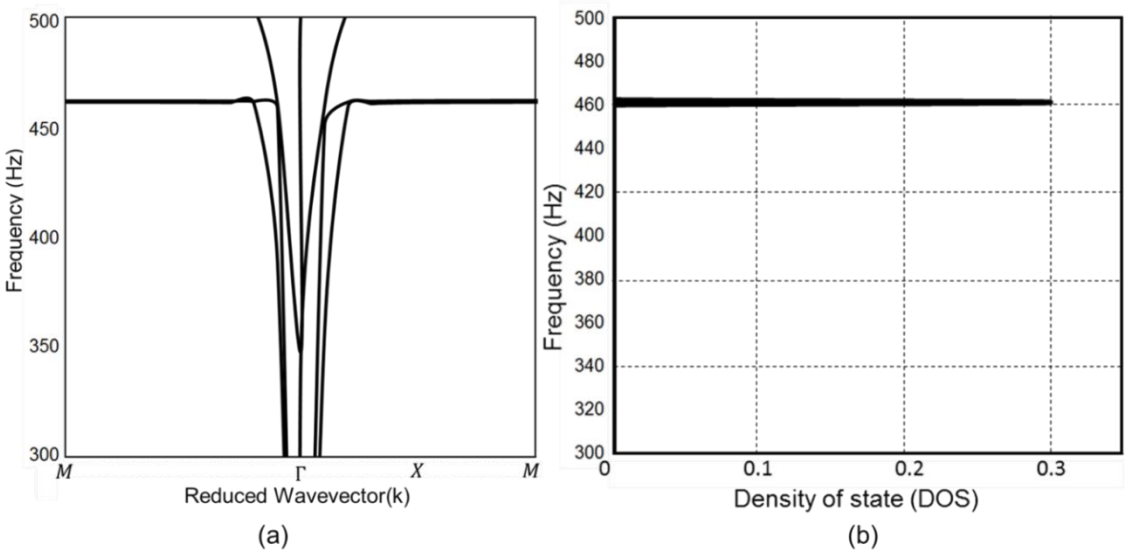

Figure-4.1: (a) Band structure of the unit AEMM and (b) density of state representation of the unit AEMM

In calculating the DOS, the total wave number $\sum dk$ is computed for each frequency with frequency step $d\omega = 1Hz$[33]. Fig. 4.1(b) shows the computed DOS for the frequency range 300-500 Hz. The DOS peak at ~460 HZ corresponds to the flat band in

the dispersion plot in Fig. 4.1(a) and confirms the existence of the local resonance at ~460 HZ.

To understand the vibration pattern of the constituents at local resonance frequencies, modal displacements of the unit cell is investigated. Fig. 4.2 shows the displacement profiles at two DOS peak frequencies (460 Hz & 461 Hz). It can be seen that, at both the local resonance modes, the core mass is resonating, and the acoustic energy is trapped inside the matrix constituent of the cell as dynamic strain energy. It has also been noticed that both the vibration modes are 90^0 mirror images of one another. Which confirms that both the modes representing same vibration mode and only one local resonance frequency exist at ~461 Hz. Hence, it can be concluded that using unit cell AEMM with proposed mechanical and geometric configurations; it is possible to trap acoustic energy at ~460 Hz inside the AEMM. Section 4.3 provides a clear insight; how much acoustic noise can be filtered through such energy trapping process.

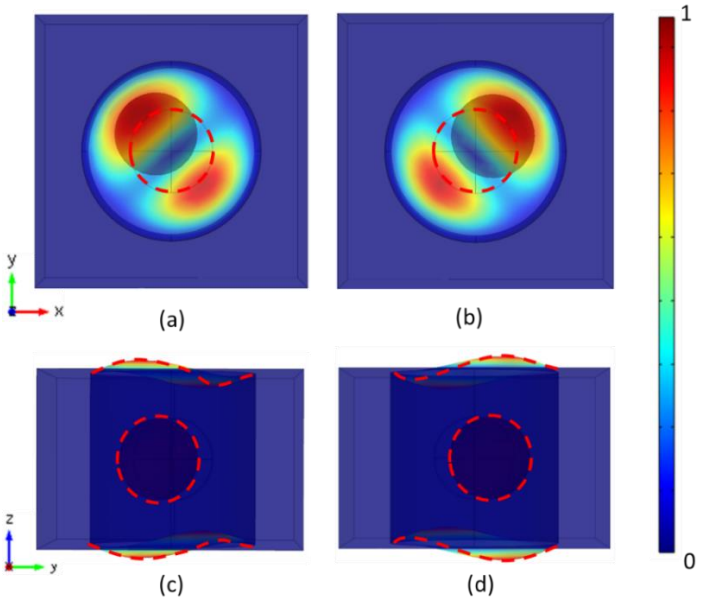

Figure-4.2: Displacement plot of a unit cell of the MetaWall at (a) Top view of the cell at 460Hz (b) Top view of the cell at 461Hz (c) side view of the cell at 460Hz (d) side view of the cell at 461Hz

4.2 Analytical Study

While the numerically computed outcomes in the previous section confirm the existence of local resonance mode and the possibility to trap acoustic energy in unit cell AEMM at ~460 Hz, an analytical study is performed herein to validate the numerical claims. The unit cell AEMM can be evaluated as a spring-mass system as shown in Fig-4.3(a).

For analytical validation, a one-dimension system is assumed for two principal purposes, 1) computation simplicity, and 2) cell constituent's deformation in other dimensions are neglected since unidirectional acoustic incidence is assumed. Based on the assumptions, the dynamic effective mass of the microstructures can be presented as

$$M_{eff} = M_0 + \frac{2Km_1}{2K - m_1\omega^2} \quad \text{...(1)}$$

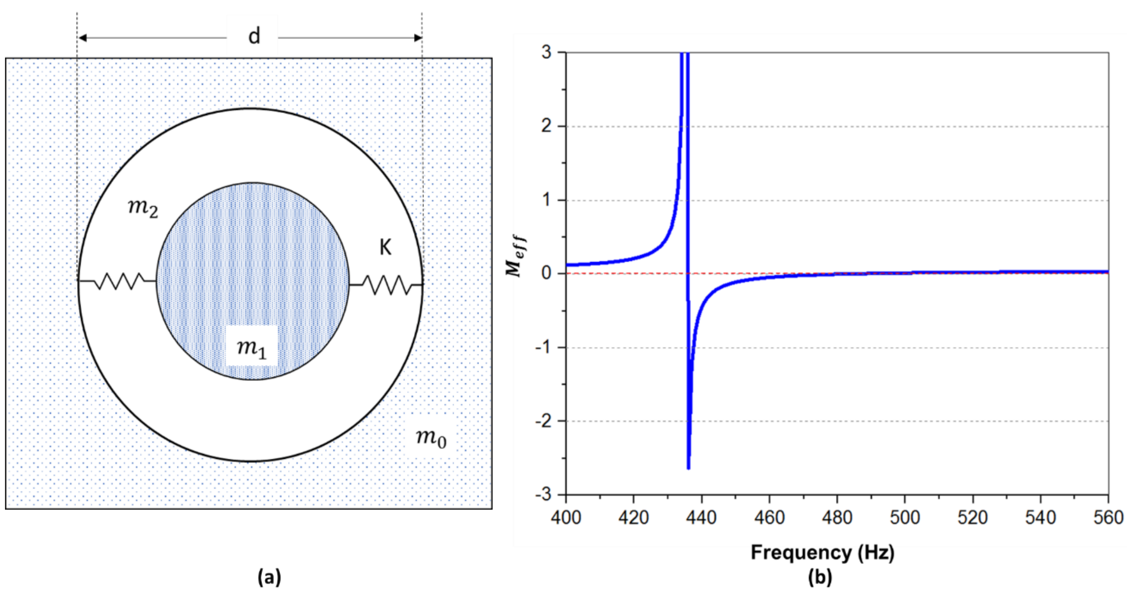

Figure-4.3: (a) Spring-mass representation of unit cell AEMM (b) Analytically computed dynamic effective mass of the AEMM

Here, M_0 and m_1 are the masses of concrete frame and lead core, respectively. The spring constant for the matrix component is counted as, K = 1 kPa. From Equation (1), the dynamic effective mass of the system is found to be negative at ~440Hz, as shown in Figure 4.3(b), which can be counted as local resonance frequency according to the established literature[34]. While ~460 Hz is recorded as the local resonance frequency of the unit cell AEMM, a little deviation is measured in analytical computation due to the adaptation of assumptions as mentioned above. Hence, it can be claimed that, the analytical study supports the numerical computer in a good degree.

4.3 Filtration of Acoustic Energy

Based on the above discussions, it is evident that under any vibroacoustic loading condition, the AEMM unit cell can trap acoustic energy at a specific frequency inside the soft matrix due to their unique material properties. However, the capability of the AEMM MetaWall as noise filter through such energy trapping is yet to be tested. A MetaWall placed in highways or industries are not only exposed to increased acoustic pressure, but also environmental ground vibration. This vibration is generated due to the vibroacoustic waves originated from the movement of traffic or vibration of heavy industrial machinery under operation. Hence, to demonstrate the capability of the MetaWall in filtering acoustic pressure, a virtual experiment is created using COMSOL Multiphysics.

A frequency domain analysis is performed applying unit pressure (~94dB) at the boundary of the incident acoustic domain (ref.Fig.-4.4(a)). To consider the input load as acoustic pressure, a long air duct of length L is designed at both input and receiving ends of the AEMM (Fig. 4.4(a)).

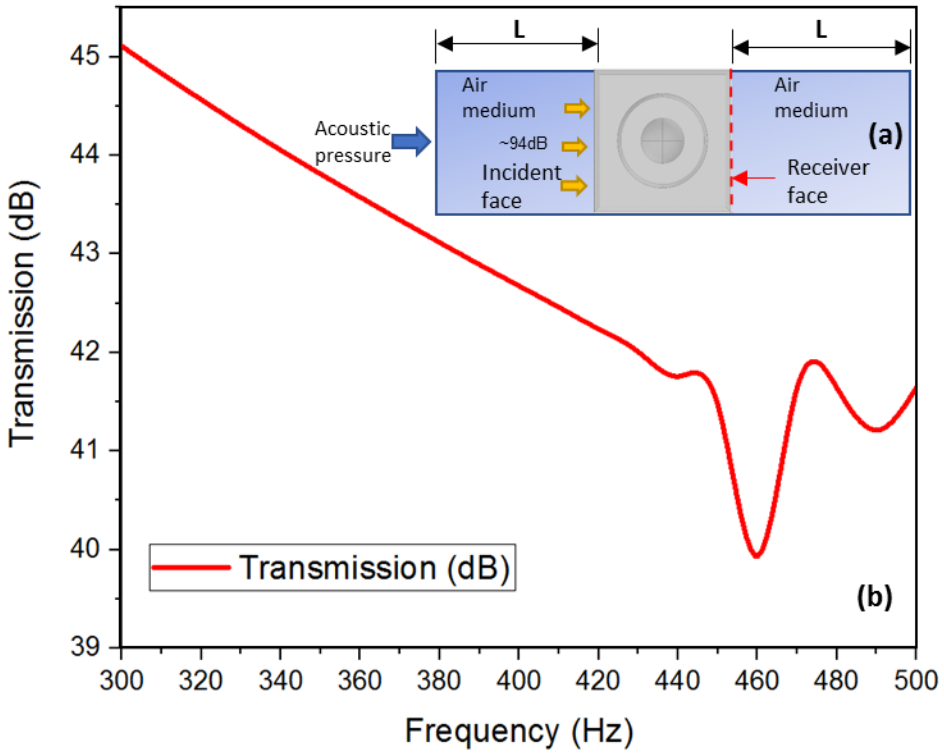

Figure-4.4: (a) Acoustic pressure test setup; (b) Filtration of the acoustic noise in the matrix

L is defined as twice the wavelength with respect to the maximum frequency studied in the air medium. Fig. 4.4(b) shows the acoustic pressure level at the receiver surface of the AEMM for a range of acoustic frequencies. A drop in acoustic pressure amplitude (dB) is visible for all the frequencies at the receiving end, compared to the incident 94dB pressure. However, a significant drop of around ~57.7% is recorded in the vicinity of the resonance frequency. Hence, this study confirms AEMM MetaWall as potential noise barrier with almost ~60% noise reduction capability.

CHAPTER 5

AEMM MODEL AS ENERGY HARVESTER

5.1 Potential use of the Filtered Acoustic Energy

Since acoustic energy is trapped inside the metamaterial in the process of filtering noise, it is possible to recover this abundant energy as usable electric potential[27]. Two piezoelectric material types (ceramic wafer and PVDF) were considered independently inside the unit cell AEMM to convert the trapped strain energy into electric power (Ref. Fig. 4.1(a)).

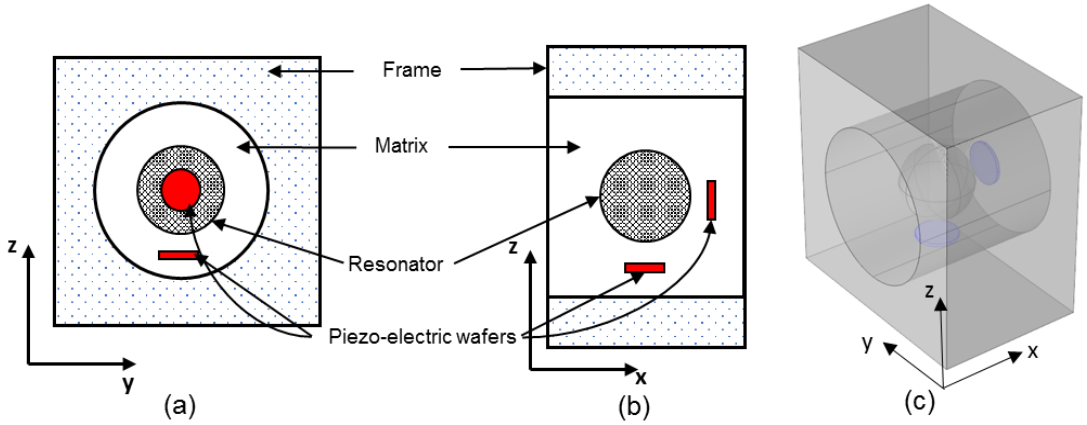

Figure-5.1: Placement of the piezoelectric wafers or PVDF membrane to maximize power output (a) plan view and (b) side view; (c) proposed piezoelectric material placement in a unit cell to harvest energy from the resonance mode

Harvesting energy from AEMM at different vibration modes has already been reported in previous articles [35]. To harvest the maximum possible energy trapped inside the cell, strategic placements of the energy conversion material inside the soft-core constituents of the AEMM is important. Each local resonance mode arrests the dynamic wave energy inside the matrix constituent of the cell. Hence, it is expected that appropriate placement of an energy conversion material, capable of mechanoelectrical transduction, with proper design of the matrix component can provide a significant electric potential at the local resonance frequencies. Fig. 5.1(a,b) shows the proposed placement of the piezoelectric material in the unit cell. It has been found that in unit cell AEMM, after placing PZT (7mm Dia. And 0.5mm thickness) inside the cell, there are always two dominant vibration or local resonance modes exist, 1) core mass resonated along the axis of excitation, 2) core mass resonated along the thickness axis of PZT, unless the thickness axis is making a right angle with axis of excitation. One additional vibration mode with little dominance is also identifiable along the gravitational (z-) axis of the resonator. It is possible to have maximum power from a PZT if all three vibration modes coincide. However, due to application compatibility, in this work, it's not possible to coincide axis of excitation and gravitational axis. Hence, two piezoelectric wafers are proposed herein to extract the maximum power from the unit cell AEMM. While one PZT will coincide the axis of excitation and PZT thickness axis, the other PZT will generate power due to the gravitational effect of the core resonator (Ref. Fig. 5.1). In all the above cases, PZT is placed in the middle of core surface and frame inside the boundary.

On the other hand, similarly at similar locations, PVDF materials of same dimensions (7 mm. dia.) were placed (except the thickness was 100μm). When the PVDF

material was used only one resonance frequency was found due to the core mass only in the AESC. However, the energy output of the PVDF membrane from the MetaWall was 66% higher compared to the PZT around the ~460 Hz. It was found from an analysis using a single AESC unit that higher surface area of the PVDF in a cylindrical configuration around the resonator could result in much higher energy output, but the resonance frequency was well above the specified limit of application which is below 500 Hz considered herein. Hence, such configurations of the PVDF membrane inside AESC are not reported in this article but might be suitable for different applications. The material properties for PZT-5H (density 7500 kg/m3) and PVDF (density 1780 kg/m3) used in the simulation written in the following equations

PZT-5H Compliance Matrix:

$$S = \begin{bmatrix} 16.5 & -4.78 & -8.45 & 0 & 0 & 0 \\ -4.78 & 16.5 & -8.45 & 0 & 0 & 0 \\ -8.45 & -8.45 & 20.7 & 0 & 0 & 0 \\ 0 & 0 & 0 & 43.5 & 0 & 0 \\ 0 & 0 & 0 & 0 & 43.5 & 0 \\ 0 & 0 & 0 & 0 & 0 & 42.6 \end{bmatrix} \times 10^{-12}\, Pa^{-1} \quad \text{..... (2)}$$

PZT-5H Piezoelectric charge constants or the coupling matrix:

$$d = \begin{bmatrix} 0 & 0 & 0 & 0 & 741 & 0 \\ 0 & 0 & 0 & 741 & 0 & 0 \\ -274 & -274 & 593 & 0 & 0 & 0 \end{bmatrix} \times 10^{-12} C/N \quad \text{..... (3)}$$

PZT-5H Relative permittivity matrix:

$$\varepsilon = \begin{bmatrix} 1704.4 & 0 & 0 \\ 0 & 1704.4 & 0 \\ 0 & 0 & 1433.6 \end{bmatrix} \quad \text{..... (4)}$$

PVDF Compliance Matrix:

$$S = \begin{bmatrix} 4.06 & -5.09 & -10.12 & 0 & 0 & 0 \\ -5.09 & 2.20 & -8.75 & 0 & 0 & 0 \\ -10.12 & -8.75 & 15.28 & 0 & 0 & 0 \\ 0 & 0 & 0 & 1.82 & 0 & 0 \\ 0 & 0 & 0 & 0 & 1.69 & 0 \\ 0 & 0 & 0 & 0 & 0 & 1.43 \end{bmatrix} \times 10^{-12}\, Pa^{-1} \quad \text{..... (5)}$$

PZT-5H Piezoelectric charge constants or the coupling matrix:

$$d = \begin{bmatrix} 0 & 0 & 0 & 0 & -0.137 & 0 \\ 0 & 0 & 0 & -0.126 & 0 & 0 \\ -0.93 & -0.67 & 2.8 & 0 & 0 & 0 \end{bmatrix} \times 10^{-12} C/N \quad \text{..... (6)}$$

PZT-5H Relative permittivity matrix:

$$\varepsilon = \begin{bmatrix} 12 & 0 & 0 \\ 0 & 12 & 0 \\ 0 & 0 & 12 \end{bmatrix} \quad \text{..... (7)}$$

In Fig. 5.1, the placement of piezoelectric materials to harvest energy at the frequency ~460Hz is proposed. Hence, to verify the concept of transforming the trapped acoustic energies into usable electric potential, the model is numerically simulated using COMSOL Multiphysics. In the model both type of piezoelectric materials namely, PZT and PVDF materials were used, independently. As described in the introduction section, two arrangements of MetaWall (concrete free-surface and matrix free-surface) are proposed in order to change the incident face of the brick and observe the change in our expected output. Both configurations were tested with both types of piezoelectric materials. In concrete free-surface setup, the concrete frame of each unit cell remains as the free surface to experience the direct acoustic incidence. In case of matrix-free surface configuration, the unit cell is rotated, and the surface with matrix constituent of the cell will be exposed. Multi-layered MetaWall can be a practical choice for industrial application for robustness and improved performance with required compressive strength. In case of matrix-free surface arrangement, if the bricks are placed right one after another, the matrix constituent will be continuous along the whole thickness and could not feel any resistance to experience sufficient strain. Such arrangement may reduce the local strain energy and total power output. Hence, a capping mechanism is envisioned to enhance the local strain

energy in each cell. Both single and double cover configurations are considered, where, a reasonable gap is considered in between two adjacent layers in case of a single cover design.

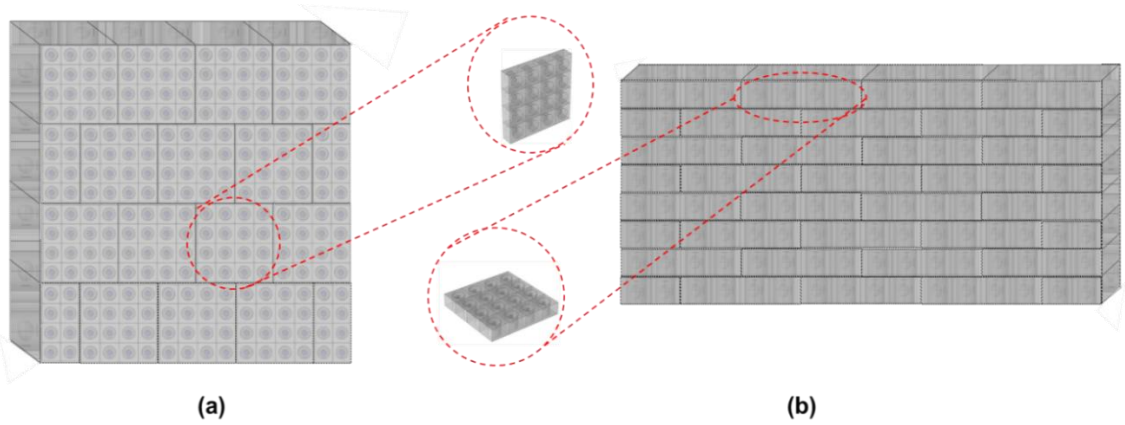

Figure-5.2: Two different arrangements of the MetaWall brick (a) concrete free surface arrangement (b) matrix free surface arrangement

Such gap is important to distinguish between single and double capping, as well as keeping the local resonance frequency for the whole MetaWall brick consistent. It was found that any arbitrary arrangement of capping was not suitable, and the resonance frequency might go well above 500 Hz and is not desired. With the capping arrangement proposed herein, the resonance frequency was very close and right around ~500 Hz with both single and double cover case. Capping arrangement will be fruitful for both types of piezoelectric materials. Though, a multilayer MetaWall arrangement is important for the industrial application, for computation simplicity, in this work, a single layer brick with 16-cell AESC are investigated.

5.2 Concrete Free Surface Arrangement

As conceptualized and proposed, the model is placed in such a way that the concrete frame of the unit cell remains as the free surface of the MetaWall. Here, displacement boundary condition is applied along the thickness direction of the MetaWall to simulate effective acoustic and ground vibration. Hence, matrix surface remains parallel to the axis of excitation. Also, the direction of the excitation coincides one piezoelectric material (PZT or PVDF as used) placed in the unit cell.

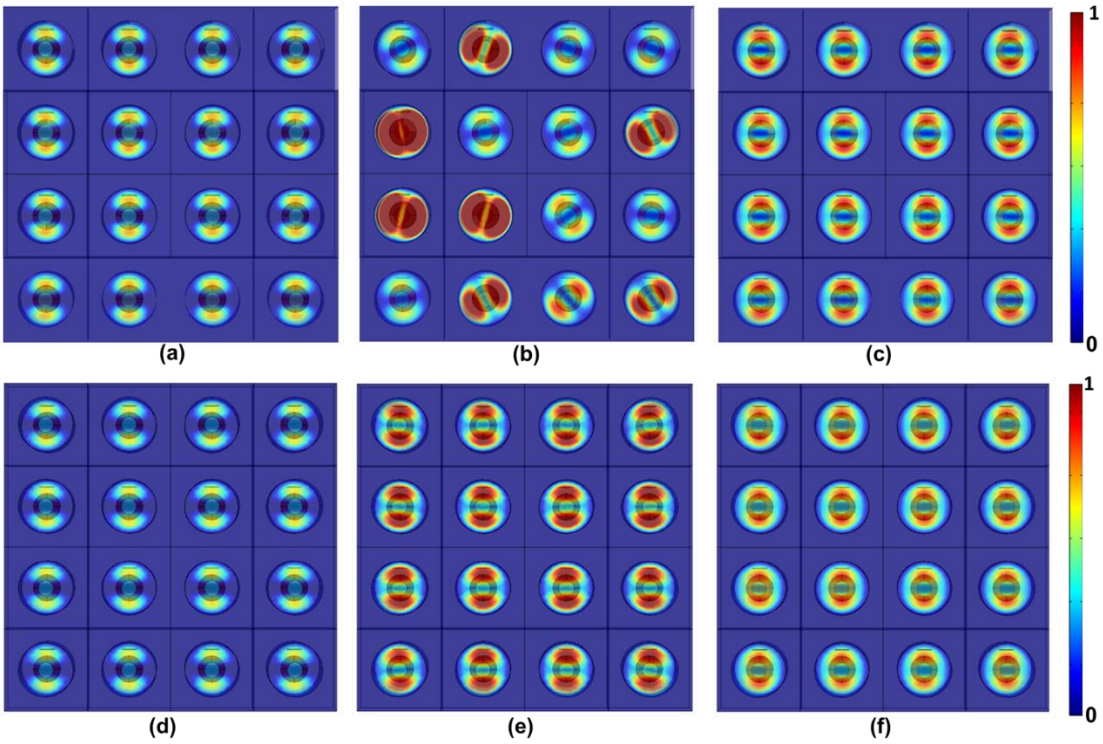

Figure-5.3: Displacement plot at frequency (a) f_1(420Hz) (b) f_2(458Hz) (c) f_3(490Hz) using PZT and displacement plot at frequency (d) f_1(420Hz) (e) f_2(458Hz) (f) f_3(490Hz) using PVDF

The displacement plots of the respective cells at three different frequencies around ~420 Hz, ~460Hz, and ~490Hz using both PZT and PVDF materials are shown in Fig 5.3. At local resonance frequency around ~460 Hz, it can be seen that maximum strain energy is trapped inside the matrix constituent with PZT and PVDF material as shown in Fig-5.3(b) & Fig-9(e), respectively. Hence, the PZT and PVDF piezoelectric materials experienced maximum compressive and bending stress, which resulted in maximum power output (~1.3mW from PZT and ~2.1mW from PVDF) as presented in Fig.-5.4 (a) and (b), respectively. While a local resonance frequency of ~460 Hz was reported in earlier sections from eigenfrequency analysis, a little shift is recorded in this section due to the addition of an extra mass (PZT) in the unit cell.

5.3 Matrix Free-Surface Arrangement

In another arrangement of the MetaWall with the matrix-free surface, the model is placed in such a way that the matrix surface remains perpendicular to the axis of excitation. In this arrangement of the bricks, two configurations are considered. In the first configuration, the MetaWall has a thin layer of cover on both sides of the concrete frame which was originally considered open to the atmosphere in other arrangements (See Figure 11(b)). This type of arrangement is chosen in order to fulfill the requirement of a wall with multiple layers of brick. The ones which will be in the middle layers will have both its faces covered by other layers.

In another setup, cell cover is considered on one face of the unit cell, preferably on the side where the piezoelectric wafers are placed on top of the resonator (see Figure 11(a)). In the arrangement, when the covers are placed on both sides, the resonance frequency was

found to be higher (~508HZ) compared to the resonance frequency of the wall without a cover (~460Hz) (ref. Fig -5.8). On the other hand, for the arrangement that has a one-sided cover, the resonance is reported at a higher resonance frequency (~500Hz), which is comparatively lower than the frequency reported with double-sided covers on the MetaWall (~508Hz). Adding cover in the cell makes the soft rubber stiff and leaves very little room to deform. Hence, with double cover resonance frequency shifted to higher frequency compared to the cell with a single cover.

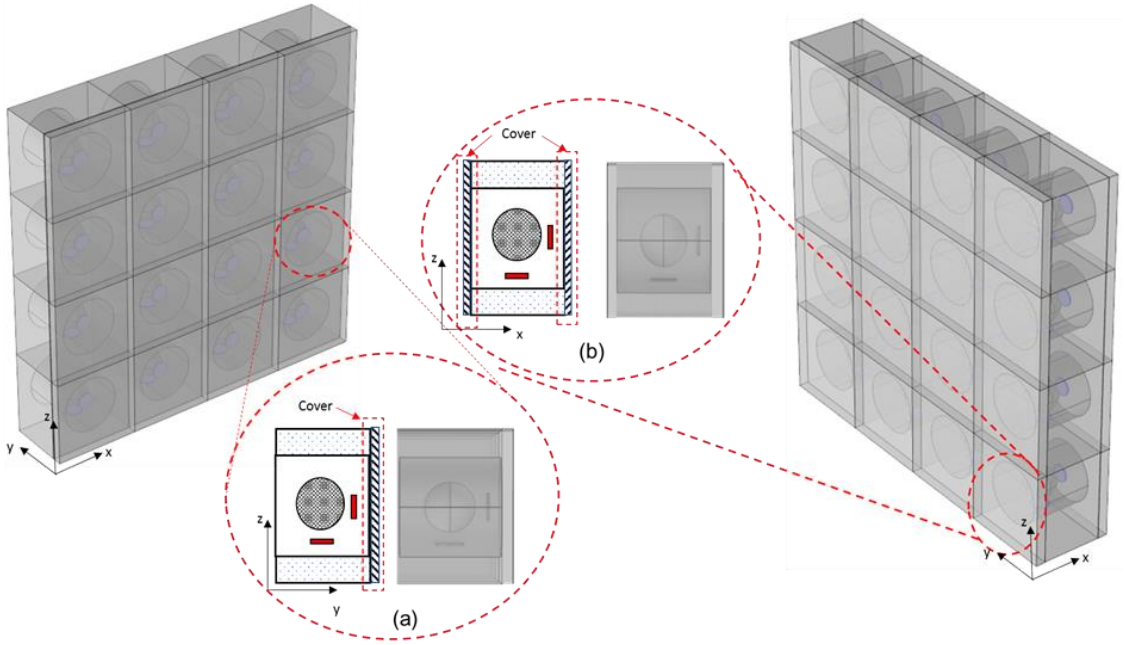

Figure-5.4: Illustration of a unit cell of MetaWall brick with (a) single cover; (b) double cover

5.4 Experimental Process

In this section, the concept of harvesting energy from the concrete free-surface model of the AEMM MetaWall brick is experimentally validated. A full-scale MetaWall

brick is fabricated in the laboratory and the fabrication steps are discussed as follows. First, the cylindrical acoustoelastic sonic crystals are fabricated using an established method reported by Ahmed et al. [29] with few additional steps discussed in this section.

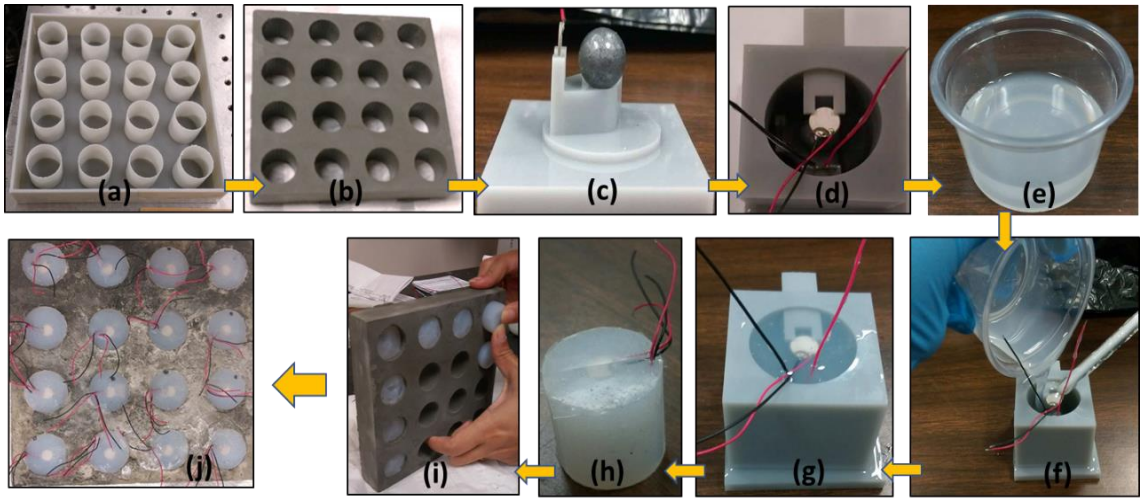

Figure-5.5: (a-i) Fabrication steps of the MetaWall brick (j) the final form of the brick

To fabricate the concrete structure, a mold is first designed and then fabricated using 3D printing technology (Fig. -5.5(a)). Portland cement concrete mortar mix prepared with water in a 0.5/0.5 mixing ratio is used to build the structure. A cylindrical support to place the resonator ball was fabricated using 3D printing technology in between the energy transduction units and the pins for holding the piezoelectric wafers in their designated places. The mold for making the harvesters is shown in Fig.-5.5(d). After the placement of the lead resonator and the wafers, liquid rubber (Mold star 20T, contains two parts (A & B)), is used to fill the hole in 3D printed block. Since it is necessary to sense or transfer the strain energy trapped inside the rubber component, the piezoelectric wafers (with electric wires) were fully submerged into the liquid rubber in such a way that it remains

untouched by both the lead balls and the mold. It is important to keep the piezoelectric wafers straight. The rubber used in this process has a curing time of 30 mins. During the initial steps, the cylindrical support and the pins are used to hold the lead ball and the piezoelectric wafers in the middle. So, empty spaces remained at the bottom of the structure after removing the cylindrical support. Another cavity is created after the removal of the top pin.

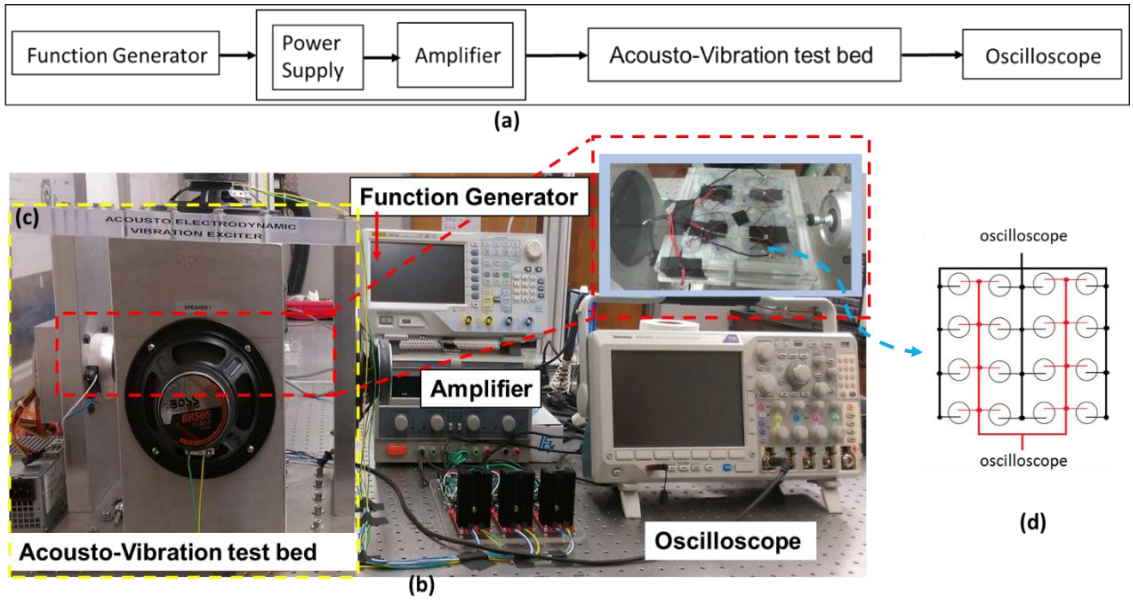

Figure-5.6: (a) Sequence of the experimental process to harvest energy from the vibration test bed (b) Experimental configuration of MetaWall brick to harvest energy (c)Customized acousto-vibration test bed (d) circuit diagram of the parallel connection used to connect the piezoelectric wafers embedded in the unit cells.

Further, these empty spaces were filled with additional rubber following the same procedure described above. Since it is required to have a good bonding between the two layers of rubber, the second step needs to start before the full curing of the rubber poured first. After the curing process, the energy harvesters look like the one shown in Fig.-5.5(h).

All 16 sonic crystal harvesters are made in the same process. Once all the crystals are completed, they are inserted into the cylindrical hole in the concrete frame (Fig.-5.5(i)) of the MetaWall. Then, the MetaWall brick is ready for the experimental investigation (Fig. -5.5(j)).

A customized 3D acousto-vibration testbed[36] is used to perform the experiments. The vibration testbed is shown in Fig. 5.6(b). The voltage output from the piezoelectric wafers is captured in parallel connection across a 10 KΩ resistive load and power density is calculated. The circuit diagram for connecting the wafers in parallel connection is displayed in Fig. 5.6(c).

5.5 Results and Discussion

Hence, the PZT and PVDF piezoelectric materials experienced maximum compressive and bending stress, which resulted in maximum power output (~1.3mW from PZT and ~2.1mW from PVDF) as presented in Fig.-5.7(a) and (b), respectively. While a local resonance frequency of ~460 Hz was reported in earlier sections from eigenfrequency analysis, a little shift is recorded in this section due to the addition of an extra mass (PZT) in the unit cell.

The displacement plots of the respective cells at three different frequencies at 420 Hz, 458Hz, and 490Hz. are shown in Fig.-5.3. At local resonance frequency, 458 Hz, it can be seen that maximum strain energy is trapped inside the matrix constituent (ref. Fig-5.3(b), (e)). Hence, the piezoelectric wafers experience maximum compressive stress, which resulted in maximum power (~1.2mW from PZT and 2.1mW from PVDF) output as can be seen from Fig.-5.7. While a local resonance frequency of ~460 Hz was reported in earlier

sections from eigenfrequency analysis, a little shift is recorded in this section due to the addition of an extra mass (PZT and PVDF) in the unit cell.

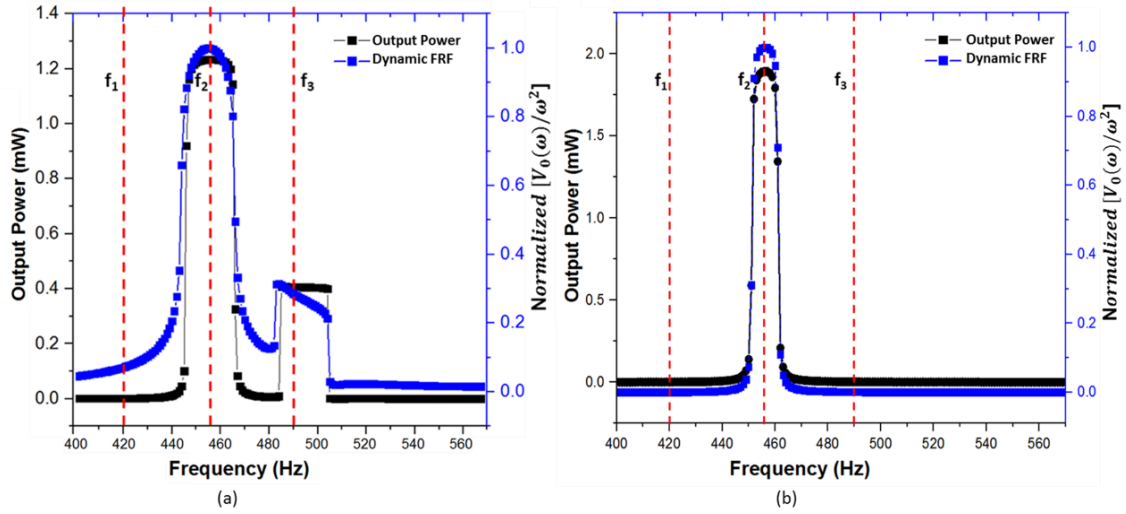

Figure-5.7: Power output and normalized voltage output from (a) a single layer of the multi-layer MetaWall model with PZT (b) a single layer of the multi-layer MetaWall model with PVDF

To simulate the possible power output from the MetaWall using PZT and PVDF independently, 10KΩ resistive load was added to the models. The maximum power harvested by PZT from a MetaWall with a double-sided cover arrangement was found to be around ~5.7 mW, and with the single sided cover was around ~8.8mW. Similarly, the maximum power harvested by PVDF from a MetaWall with a double-sided cover arrangement was found to be around ~2.5 mW, which is significantly lower than the PZT. However, with the single sided cover arrangement the harvested power was ~30% higher and was around ~11.5mW with PDVF compared to PZT based walls. It was found that the resonant frequencies, however, were around ~485 Hz and ~530 Hz, respectively. Generally

speaking, the power harvested from a single covered MetaWall is significantly higher than the one with a double cover MetaWall. Since in double cover configuration, the matrix constituent is capped from all sides and enclosed in a closed space, the constituent can experience less deformation compared to the cell with just one side capped. Hence the piezoelectric wafer inside the double cover cell experiences less strain and results decreased power output compared to the model with a single cover. Fig. 5.8(a) shows the power output from single and double cover wall using PZT and Fig. 5.8(b) shows the power output from single and double cover wall using PVDF. This concludes that if the double-sided cover is absolutely necessary, embedding PZT would be beneficial compared to PVDF. From the numerical study, ~1.2mW maximum power was recorded from the entire brick upon unit displacement (1 mm) excitation when the PZT was used as the smart material inside the harvester. Fig. 5.9 shows the experimental power output curve obtained from several experiments. It can be seen that the mean experimental power output is ~0.45mW near ~490Hz. While the numerical power output is ~1.2mW around the frequency (~460Hz). Error bar (only positive error bars are shown) with one standard deviation in Fig. 5.9 shows that the maximum power output could be ~0.55 mW from the wall that was fabricated in the laboratory. Another observation can be made that the standard deviation is higher towards the lower frequencies compared to the higher frequencies above ~490 Hz. The result shows that at close proximity to ~460 Hz, at 490 Hz < 500 Hz, the maximum power could be harvested from the MetaWalls, while retaining their compressive strength as desired in a structural material.

The result closely supports the analytical and numerical argument which says that the maximum power is to be obtained around ~460 Hz. However, a 30Hz shift in the

resonance (or, peak power output) frequency is the result of many factors. Primarily this mismatch is due to the fabrication error, placement of the resonators, the exact inclination of the piezoelectric wafers which might have tilted during pouring the rubber into the mold and concrete strength after curing, etc.

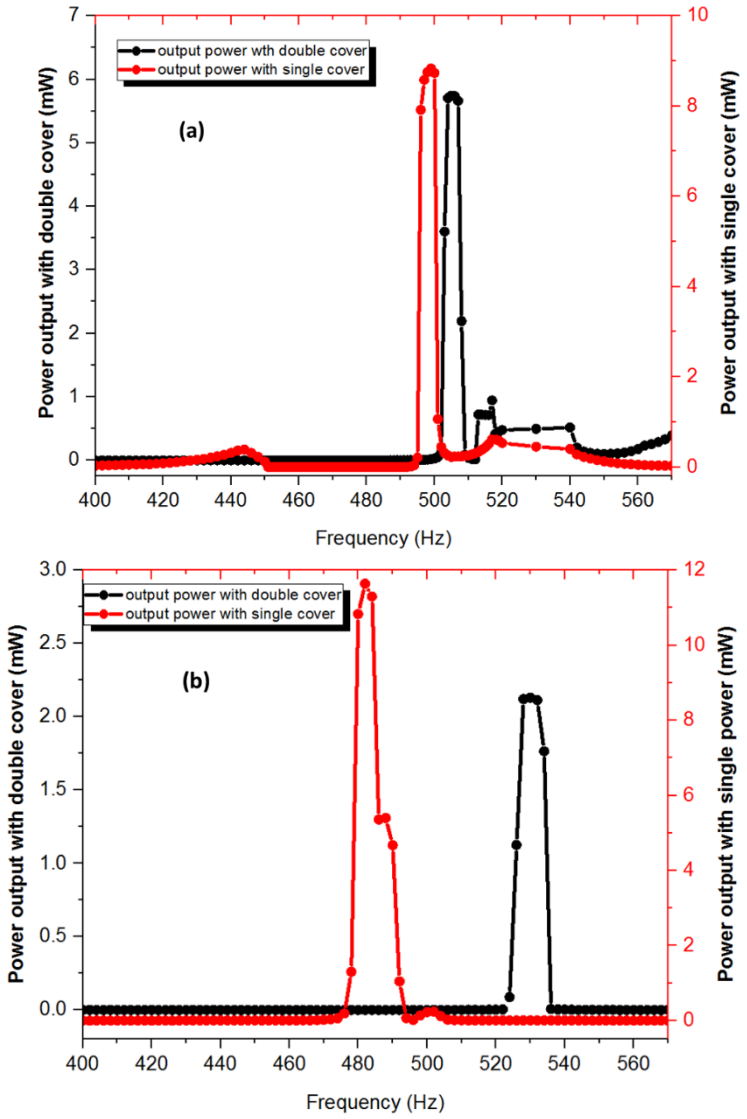

Figure-5.8: a) Power output in vertical arrangement with cover on both sides and with single cover using embedded PZT, b) Power output in vertical arrangement with cover on both sides and with single cover using embedded PVDF

The material properties of the concrete used are provided by the vendor, which is used in the simulation and might not exact. However, after curing the small perturbation in the material properties of the core structure may have shifted the resonance frequency which is previously investigated [13].

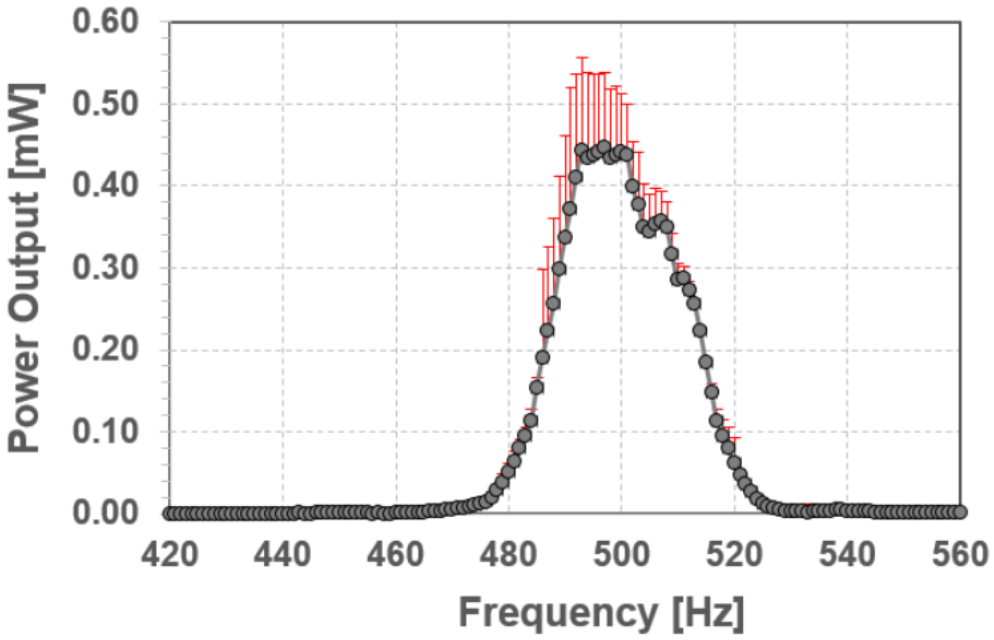

Figure-5.9: Experimental power output from the proposed model

A similar argument holds true for the maximum power output which is close to 50% of the simulated power output. A similar investigation was conducted on the MetaWall brick with embedded PVDF of the same size. Although the numerical simulation results in higher power output compared to PZT based MetaWall, ~2.1 mW, the energy output from experiments were not promising (~0.22 mW) and inconsistent between a different set of experiments, hence, not reported herein. This is not to report that the PVDF

cannot work for MetaWalls but requires different fabrication process by virtue of which the higher energy output could be achieved as predicted in Fig.5.7(b) and 5.8(b). This is primarily due to the difficulty in fabricating the PVDF based MetaWalls using the process described above. However, a different optimized process could result in a better fabricated product of MetaWall with PVDF, which is not reported or investigated in this article.

CHAPTER 6

POWER REQUIREMENTS FOR NDI SENSORS

6.1 Basics of Nondestructive Inspection (NDI) testing

Nondestructive inspection (NDI) is the process of inspecting, testing, or evaluating materials, components or assemblies for discontinuities, or differences in characteristics without destroying the serviceability of the part or system. In other words, when the inspection or test is completed the part can still be used. The destructive tests are often used to determine the physical properties of materials such as impact resistance, ductility, yield and ultimate tensile strength, fracture toughness and fatigue strength, but discontinuities and differences in material characteristics are more effectively found by NDI. Ultrasound is the commonly used technique in NDI to detect the presence of defects or determine the elastic properties of materials. Typically, transducers with frequencies between 1 and 10 MHz are used in production NDI.

6.2 Available Actuators/Sensors in Market for NDI Operation

In this report, we have investigated some of the commercially available ultrasonic transducers/sensors for NDI operation. The frequency of usual transducers ranges from 20 kHz to couple of MHz. However, in this investigation, transducers with a frequency range around ~5 MHz is only considered, since, those can be driven by portable batteries. Apart from battery, AC power driven transducers can also be found on the market. However, since, in this project, the NDI sensors/transducers are aimed to power through energy

harvesting technology, battery-driven devices are considering, evaluating compatibility issue. An energy harvesting circuit can easily be coupled to a portable battery.

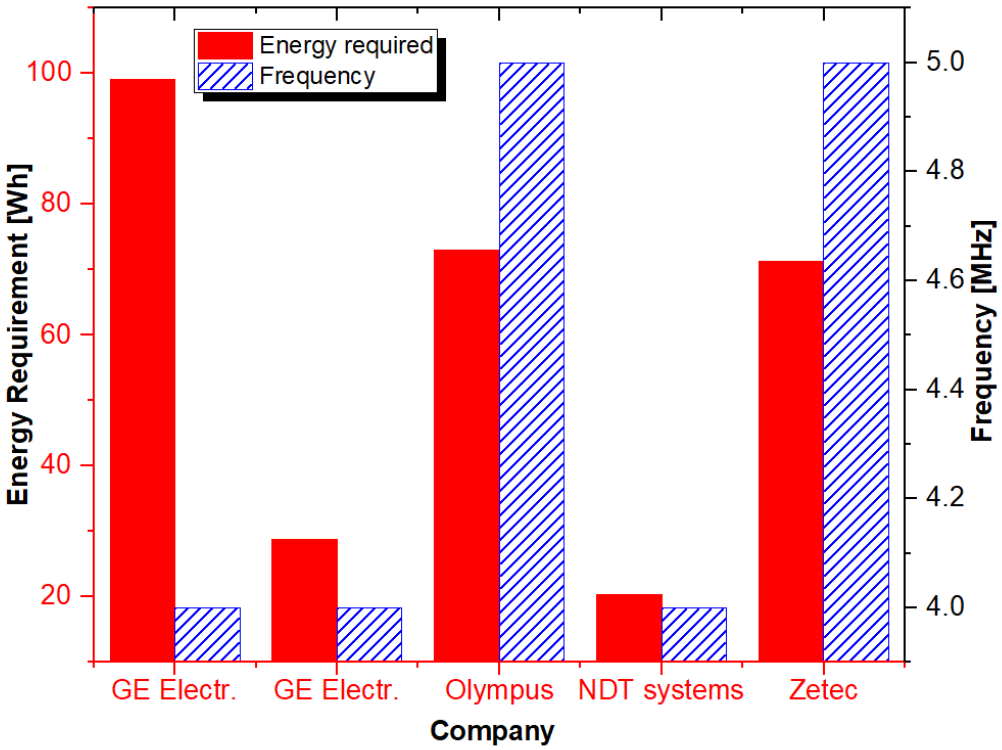

Figure-6.1: Power requirement of transducers manufactured by different companies.

The data presented in the chart is tabulated in Table-6.1 From the table it can be seen that transducers from different company require different energy level to operate for one hour, ranging from ~20Wh to ~100Wh. Arbitrarily, if transducer from Olympus is chosen to employ in NDI operation, it may require ~73Wh of energy for one hour and ~6Wh for 5 mins of operation. According to the manual, the same transducer may require ~122mW of energy for single excitation/inspection.

While the AEMM MetaWall is providing 1.2mW of power at an instance (~ 1 sec), it can be claimed that, to make a single inspection using NDI transducer from Olympus, required power (~122mW) can be obtained running the unit AEMM wall for ~2.09min or a stack of 101 MetaWall bricks for an instance will be good enough.

Table-6.1: Power requirement of commercially available NDI transducers/sensors

Company Name	Power required	Frequency range	Type
GE electronics	99.12Wh	4MHz	Ultrasonic transducer
GE electronics	28.86Wh	4MHz	Ultrasonic flaw detector
Olympus	73Wh	5MHz	Ultrasonic flaw detector
NDT Systems	20.4Wh	4MHz	Ultrasonic transducer
Zetec	71.28Wh	5MHz	Ultrasonic transducer

Keeping the power requirement in mind, modified harvesters need to be designed. Output power from the unit cell can be improved by optimizing geometrical and material configuration in the unit cell. For this reason, some more study has been done in this field with different materials and structures.

CHAPTER 7

COMPARISON OF THE AEMM MODELS

So far we have discussed the capability of harvesting energy from AEMM cells with concrete frame and piezoelectric materials(PZT-5H and PVDF film). But there are possibilities that with the change of the frame material or the shape and size of the piezoelectric material the energy harvesting capability of the AEMM model changes. In this section, four different combination of the cells are studied.

7.1 Case Studies of the AEMM Models with Different Conditions

Here the studies are conducted on a unit cell of AEMM model. The unit cell has a dimension of (38mmX38mmX25mm). The piezoelectric materials used are PZT-5H (cylinder and disc form) and PVDF film. The frame materials used are concrete and PVC. Two orientations of the cells are considered for this study as upright and rotated(ref-Fig. 7.1). the core resonator is a lead ball. The material properties of the cell constituents are given in table-7.1. The properties of PVDF and PZT-5H are stated earlier.(ref-Chapter-5). For this study, basically, four combinations are considered, as

1. **PVDF wrap**: the PVDF film is wrapped around the core resonator.
2. **PVDF cylinder**: PVDF film is placed inside the rubber matrix in a cylinder form. The length of the cylinder is varied to see the possible outcomes.
3. **PZT-5H cylinder**: a cylinder form of the PZT-5H(dia. 6mm height 12mm) is used. The cylinder acts as both the resonator and the piezoelectric material. PVDF cylinder is also coupled with this PZT cylinder in one of the cases.

4. **PZT-5H disc and PVDF cylinder:** PVDF in the form of cylinder coupled with PZT-5H discs are considered. The lead ball acts as a core resonator.

All these cases are studied with concrete and PVC frame. The orientation of the frame was changed from upright to rotated for each case. The cases are shown in details in table 7.2.

Table-7.1: Material properties of the cell constituents

Material	Concrete	PVC	Lead	Rubber
Young's Modulus (Pa)	$11.2X10^9$	$25X10^6$	$14X10^9$	$0.9942X10^6$
Poisson's ratio	0.20	0.40	0.42	0.47
Density(Kg/m^3)	2010	1420	11350	1600

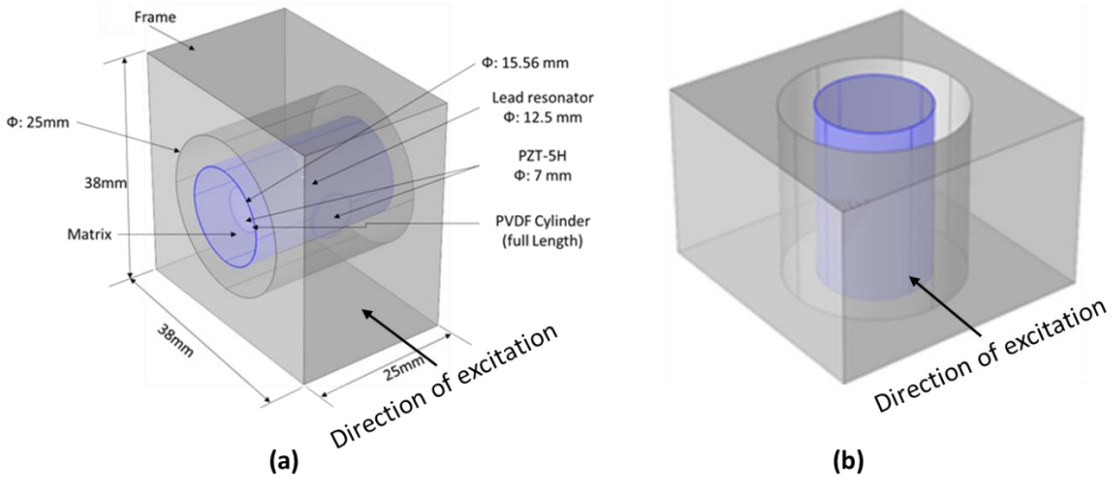

Figure-7.1: 3D view of the unit cell in (a) rotated (b) upright position

Table-7.2: Cases of the AEMM cell study conditions

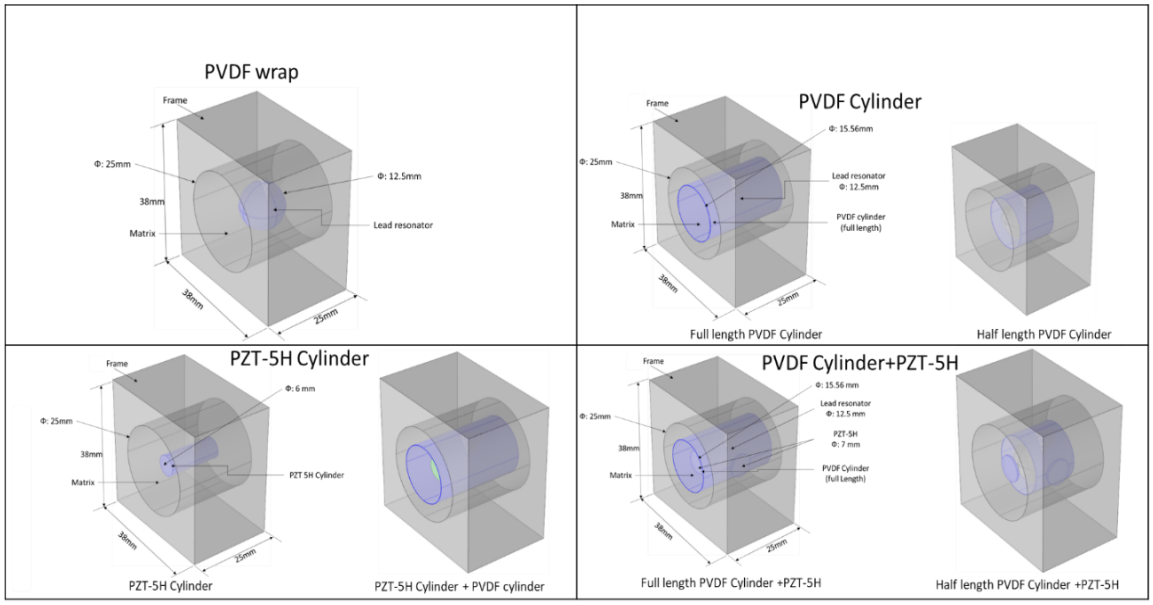

7.2 Results and Discussion

Finite element simulation tool COMSOL was used to run the simulations on these unit cells. Each of the cases with two types of orientation was simulated. The studies show that the resonance frequency and the output power differs with the frame material. Also, the output power is different with the orientation of the frame. The results are compared in table-7.3 and table-7.4 below.

From these results, it can be seen that for all of the cases, the power output is higher for the rotated orientation. The reason behind this phenomenon is the effect of the gravitational force. Apart from the applied desired excitation, this gravitational force also acts as a form of excitation. This helps to apply strain to the PVDF film or the PZT discs. So, this multi-directional strain results in higher output power. For most of the cases, the resonance frequency stays the same. A slight shift in some cases is the result of the gravitational force.

Table-7.3: Case studies with PVC frame

Serial no.	Case Studies	Power output (mW)	Resonance frequency (Hz)
1.	PVDF film wrapped around the resonator	0.0840	460
2.	PVDF cylinder (full length Cylinder)	i.Upright: 0.722 ii.Rotated: 3.622	560 600
3.	PVDF cylinder (half-length cylinder)	i.Upright: 0.25 ii.Rotated: 0.647	510 530
4.	Full length PVDF cylinder + PZT	i.Upright: 0.135 ii.Rotated: 0.694	650 650
5.	Half-length PVDF Cylinder +PZT	i.Upright: 0.014 ii.Rotated: 0.109	540 530
6.	PVDF cylinder + Cylinder PZT	i.Upright: 2.8 ii.Rotated: 3.83	720 720
7.	PZT Cylinder	i.Upright: 4.2 ii.Rotated: 3.83	560 720

From the results found from the study of the concrete frame, it can be seen that the overall power output scenario is a bit different than that of PVC frame. The power output is comparatively low compared to the same case with PVC frame. The reason behind it is the concrete frame. The density of concrete is higher than that of PVC this allows the lower

amount of deformation in the matrix. Thus, a lower amount of strain is created in the piezoelectric material. In this concrete frame also, the rotated orientation results in higher amount of output power.

Table-7.4: Case studies with Concrete frame

Serial no.	Case Studies	Power output (mW)	Resonance frequency (Hz)
1.	PVDF film wrapped around the resonator	0.2735	460
2.	PVDF cylinder (full length Cylinder)	i.Upright: 0.6708 ii.Rotated: 0.975	600 680
3.	PVDF cylinder (half-length cylinder)	i.Upright: 0.2588 ii.Rotated: 1.331	540 690
4.	Full length PVDF cylinder + PZT	i.Upright: 0.0526 ii.Rotated: 45.56	680 680
5.	Half-length PVDF Cylinder +PZT	i.Upright: 4.1717 ii.Rotated: 40.16	580 690
6.	PVDF cylinder + Cylinder PZT	i.Upright: 0.2976 ii.Rotated: 0.9396	800 800
7.	PZT Cylinder	i.Upright: 2.822 ii.Rotated: 20.767	590 800

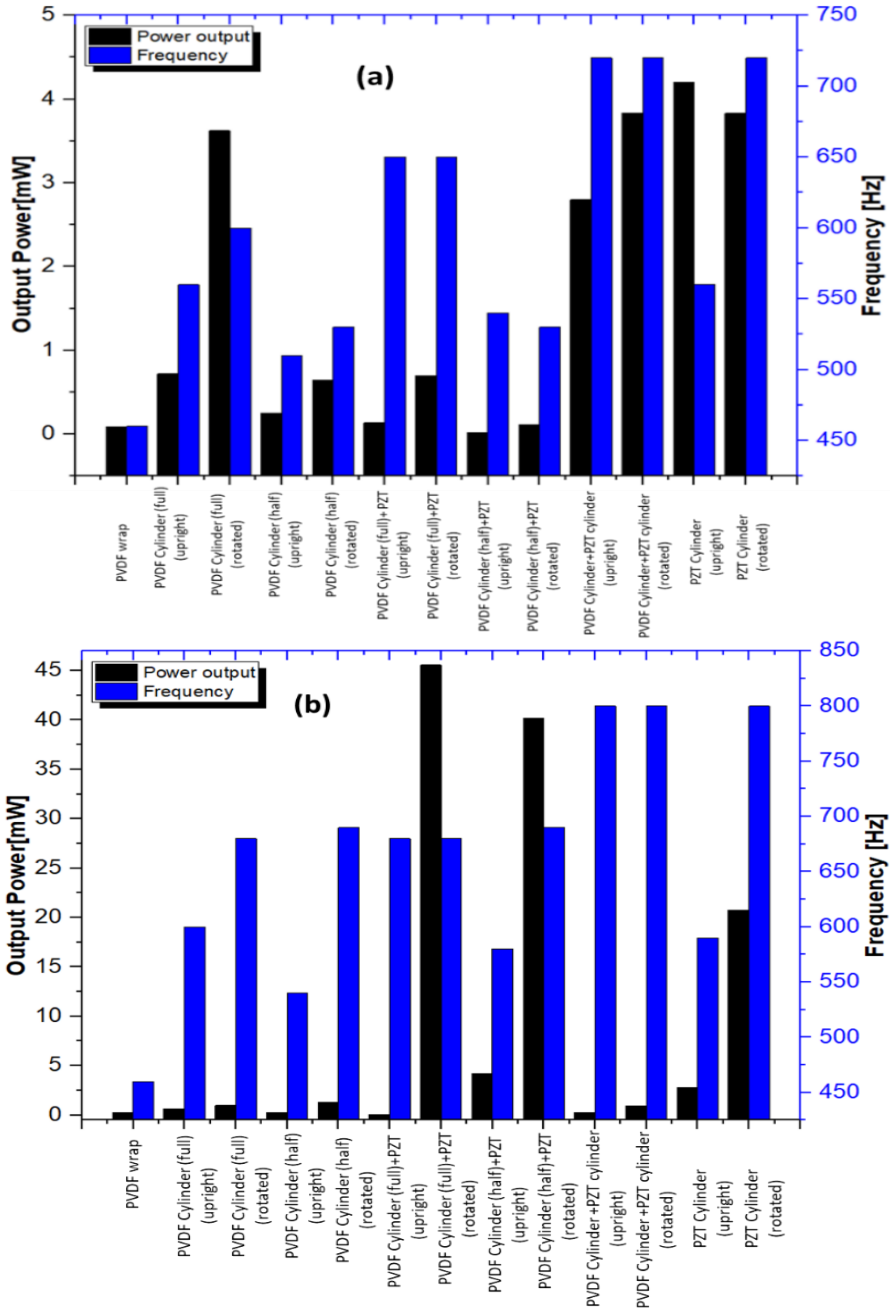

Figure-7.2: Comparison of the output power and resonance frequency with (a) PVC (b) concrete frame

The resonance frequency for the cases with the concrete frame is much higher than that of with PVC. Due to the denser frame material, the structural stiffness increases, so

the resonance frequency goes higher. Though the resonance frequencies for all the cases are lower than 1000Hz since we are looking for even lower frequency range and the weight of the structure also matters, so, the better choice for this case would be the model with PVC frame. The output power and the resonance frequency of both the frames are compared in figure-7.2.

CHAPTER 8

CONCLUSION

To summarize, this research proposes an application of the AESC based on their noise filtration capabilities. It is shown that the AESC can trap a certain frequency within its soft matrix due to its unique mechanical properties. Keeping that in mind, it has been proposed to replace the traditional roadside noise barriers with walls made of AESC. A model MetaWall brick is demonstrated that can be used to build the proposed wall. This structure helps to reduce the intensity of the annoying sound by absorbing most of the incident acoustic waves which prevent the sound to reflect back to the atmosphere. Acoustic pressure test shows that almost 60% noise attenuation is possible using the MetaWall noise barrier, where traditional barriers offer around 50% attenuation. In the process of filtering acoustic noise, an enormous amount of energy can be trapped inside AESC. Instead of leaving these energies abandoned, possible conversion in electric potential is presented, herein. It has been found that a significant amount of power output can be obtained from the MetaWall which can be used to power the street lights or SHM sensors. The scope of energy harvesting in a wide range and promising power output with minor changes in the cell constituents and its relationship with orientation is also explored. Keeping pace with the modern minimization trend, the energy harvester is proposed to be minimized to a much smaller size, as thin as a plate. The prospect, in this case, is very bright as these models can harvest smart amount of power from ambient frequency as low as 100Hz.

Finally, practical applications for power harvesting systems such as wireless sensors and self-powered units must be more evidently identified to encourage growth in this area of energy harvesting based research. This will increase the flow of ideas. With the rapid advances in low-power electronics, wireless technology, and smart structures, power harvesting is the missing link in the chain for self-powered systems.

REFERENCES

[1] H. A. Sodano, D. J. Inman, and G. Park, "A review of power harvesting from vibration using piezoelectric materials," *Shock and Vibration Digest*, vol. 36, no. 3, pp. 197-206, 2004.

[2] S. R. Anton and H. A. Sodano, "A review of power harvesting using piezoelectric materials (2003–2006)," *Smart materials and Structures*, vol. 16, no. 3, p. R1, 2007.

[3] S. Priya, "Advances in energy harvesting using low profile piezoelectric transducers," *Journal of electroceramics*, vol. 19, no. 1, pp. 167-184, 2007.

[4] C.-H. Tsai and T.-L. Wu, "A broadband and miniaturized common-mode filter for gigahertz differential signals based on negative-permittivity metamaterials," *IEEE Transactions on Microwave Theory and Techniques*, vol. 58, no. 1, pp. 195-202, 2010.

[5] C. Cianfrini, M. Corcione, and L. Fontana, "Experimental verification of the acoustic performance of diffusive roadside noise barriers," *Applied Acoustics*, vol. 68, no. 11, pp. 1357-1372, 2007/11/01/ 2007.

[6] S. Onder and Z. Kocbeker, "Importance of the green belts to reduce noise pollution and determination of roadside noise reduction effectiveness of bushes in Konya, Turkey," *Turkey. World Academy of Science, Engineering, and Technology*, vol. 66, no. 6, pp. 11-14, 2012.

[7] G. R. Watts and N. S. Godfrey, "Effects on roadside noise levels of sound absorptive materials in noise barriers," *Applied Acoustics*, vol. 58, no. 4, pp. 385-402, 1999/12/01/ 1999.

[8] M. E. Nilsson, M. Andéhn, and P. Leśna, "Evaluating roadside noise barriers using an annoyance-reduction criterion," *The Journal of the Acoustical Society of America*, vol. 124, no. 6, pp. 3561-3567, 2008.

[9] M. R. Monazzam and S. M. B. Fard, "Performance of passive and reactive profiled median barriers in traffic noise reduction," *Journal of Zhejiang University-SCIENCE A*, journal article vol. 12, no. 1, pp. 78-86, January 01 2011.

[10] X. Wang, D. Mao, W. Yu, and Z. Jiang, "Sound barriers from materials of inhomogeneous impedance," *The Journal of the Acoustical Society of America*, vol. 137, no. 6, pp. 3190-3197, 2015.

[11] M. Naderzadeh, M. R. Monazzam, P. Nassiri, and S. M. B. Fard, "Application of perforated sheets to improve the efficiency of reactive profiled noise barriers," *Applied Acoustics*, vol. 72, no. 6, pp. 393-398, 2011/05/01/ 2011.

[12] Z. Chen, B. Guo, Y. Yang, and C. Cheng, "Metamaterials-based enhanced energy harvesting: A review," *Physica B: Condensed Matter*, vol. 438, pp. 1-8, 4/1/ 2014.

[13] S. A. Cummer, J. Christensen, and A. Alù, "Controlling sound with acoustic metamaterials," *Nature Reviews Materials*, vol. 1, p. 16001, 2016.

[14] A. Can, L. Leclercq, J. Lelong, and D. Botteldooren, "Traffic noise spectrum analysis: Dynamic modeling vs. experimental observations," *Applied Acoustics*, vol. 71, no. 8, pp. 764-770, 2010.
[15] C. Buratti and E. Moretti, "Traffic noise pollution: spectra characteristics and windows sound insulation in laboratory and field measurements," *Journal of Environmental Science and Engineering*, vol. 4, no. 12, 2010.
[16] W. Choi, Y. Jeon, J.-H. Jeong, R. Sood, and S.-G. Kim, "Energy harvesting MEMS device based on thin film piezoelectric cantilevers," *Journal of Electroceramics*, vol. 17, no. 2, pp. 543-548, 2006.
[17] Z. Wang and Y. Xu, "Vibration energy harvesting device based on air-spaced piezoelectric cantilevers," *Applied Physics Letters*, vol. 90, no. 26, p. 263512, 2007.
[18] A. Erturk and D. J. Inman, "An experimentally validated bimorph cantilever model for piezoelectric energy harvesting from base excitations," *Smart materials and structures*, vol. 18, no. 2, p. 025009, 2009.
[19] Z. Chen, Y. Yang, Z. Lu, and Y. Luo, "Broadband characteristics of vibration energy harvesting using one-dimensional phononic piezoelectric cantilever beams," *Physica B: Condensed Matter*, vol. 410, pp. 5-12, 2013.
[20] S. Gonella, A. C. To, and W. K. Liu, "Interplay between phononic bandgaps and piezoelectric microstructures for energy harvesting," *Journal of the Mechanics and Physics of Solids*, vol. 57, no. 3, pp. 621-633, 3// 2009.
[21] M. Carrara, M. Cacan, J. Toussaint, M. Leamy, M. Ruzzene, and A. Erturk, "Metamaterial-inspired structures and concepts for elastoacoustic wave energy harvesting," *Smart Materials and Structures*, vol. 22, no. 6, p. 065004, 2013.
[22] H. Lv, X. Tian, M. Y. Wang, and D. Li, "Vibration energy harvesting using a phononic crystal with point defect states," *Applied Physics Letters*, vol. 102, no. 3, p. 034103, 2013.
[23] L.-Y. Wu, L.-W. Chen, and C.-M. Liu, "Acoustic energy harvesting using resonant cavity of a sonic crystal," *Applied Physics Letters*, vol. 95, no. 1, p. 013506, 2009.
[24] J.-C. Hsu, "Local resonances-induced low-frequency band gaps in two-dimensional phononic crystal slabs with periodic stepped resonators," *Journal of Physics D: Applied Physics*, vol. 44, no. 5, p. 055401, 2011.
[25] P. Sheng, X. X. Zhang, Z. Liu, and C. T. Chan, "Locally resonant sonic materials," *Physica B: Condensed Matter*, vol. 338, no. 1–4, pp. 201-205, 10// 2003.
[26] R. U. Ahmed and S. Banerjee, "Wave propagation in metamaterial using multiscale resonators by creating local anisotropy," *International Journal of Modern Engineering*, vol. 13, no. 2, p. 51, 2013.
[27] R. Ahmed, D. Madisetti, and S. Banerjee, "A sub-wavelength scale acoustoelastic sonic crystal for harvesting energies at very low frequencies (<~ 1 kHz) using controlled geometric configurations," *Journal of Intelligent Material Systems and Structures*, vol. 28, no. 3, pp. 381-391, 2017.
[28] R. Ahmed and S. Banerjee, "Predictive electromechanical model for energy scavengers using patterned piezoelectric layers," *Journal of Engineering Mechanics*, vol. 141, no. 2, p. 04014113, 2014.
[29] R. U. Ahmed and S. Banerjee, "Low frequency energy scavenging using sub-wave length scale acousto-elastic metamaterial," *AIP Advances*, vol. 4, no. 11, p. 117114, 2014.

[30] R. Ahmed, F. Mir, and S. Banerjee, "A review on energy harvesting approaches for renewable energies from ambient vibrations and acoustic waves using piezoelectricity," *Smart Materials and Structures*, vol. 26, no. 8, p. 085031, 2017.

[31] R. U. Ahmed, A. Adiba, and S. Banerjee, "Energy scavenging from acousto-elastic metamaterial using local resonance phenomenon," in *Active and Passive Smart Structures and Integrated Systems 2015*, 2015, vol. 9431, p. 943106: International Society for Optics and Photonics.

[32] G. Ma, M. Yang, S. Xiao, Z. Yang, and P. Sheng, "Acoustic metasurface with hybrid resonances," *Nature materials*, vol. 13, no. 9, p. 873, 2014.

[33] M. I. Hussein, "Reduced Bloch mode expansion for periodic media band structure calculations," in *Proceedings of the Royal Society of London A: Mathematical, Physical and Engineering Sciences*, 2009, vol. 465, no. 2109, pp. 2825-2848: The Royal Society.

[34] M. R. U. Ahmed, "Bio-inspired design of mechanical band pass sensor with the ability to scavenge energy," University of South Carolina, 2015.

[35] R. Ahmed, D. Madisetti, and S. Banerjee, "A sub-wavelength scale acoustoelastic sonic crystal for harvesting energies at very low frequencies (<∼1 kHz) using controlled geometric configurations," *Journal of Intelligent Material Systems and Structures*, vol. 28, no. 3, pp. 381-391, 2017/02/01 2016.

[36] M. Saadatzi, M. N. Saadatzi, R. Ahmed, and S. Banerjee, "An electro-dynamic 3-dimensional vibration test bed for engineering testing," in *Industrial and Commercial Applications of Smart Structures Technologies 2017*, 2017, vol. 10166, p. 101660D: International Society for Optics and Photonics.